

**PEGylated and non-PEGylated TCP-1 probes for imaging of colorectal cancer**

Zhonglin Liu,<sup>1,2\*</sup> Brian D Gray,<sup>3\*</sup> Christy Barber,<sup>1</sup> Li Wan,<sup>1</sup> Lars R Furenlid,<sup>1,4</sup> Rongguang

Liang,<sup>4</sup> Zheng Li,<sup>2</sup> James M Woolfenden,<sup>1</sup> Koon Y Pak,<sup>3</sup> Diego R Martin,<sup>1,2</sup>

<sup>1</sup>Department of Medical Imaging at College of Medicine and <sup>4</sup>James C. Wyant College of Optical Sciences, University of Arizona, Tucson, AZ

<sup>2</sup>Houston Methodist Research Institute, Houston Methodist Hospital, Houston, TX

<sup>3</sup>Molecular Targeting Technologies, Inc., West Chester, PA

**\* For correspondence or reprints contact:**

Email: [zliu@email.arizona.edu](mailto:zliu@email.arizona.edu) or [briangray@mtarget.com](mailto:briangray@mtarget.com)

**Running title:** TCP-1 molecular imaging of colorectal cancer

**Manuscript category:** Original Articles

## **Abstract**

**Purpose.** Previous studies indicate that  $^{99m}\text{Tc}$ - and fluorescent-labeled c[Cys-Thr-Pro-Ser-Pro-Phe-Ser-His-Cys]OH (TCP-1) peptides were able to detect colorectal cancer (CRC) and tumor-associated vasculature. This study was designed to characterize the targeting properties of PEGylated and non-PEGylated TCP-1 peptides for CRC imaging.

**Procedures:** Cell uptake of Cyanine7 (Cy7)-labeled TCP-1 probes (Cy7-PEG<sub>4</sub>-TCP-1 and Cy7-TCP-1) was investigated in three CRC cell lines (Human: HCT116 and HT29; Mouse: CT26). Xenografted and orthotopic CRC tumor models with HCT116 and CT26 cells were used to characterize biodistribution and CRC tumor targeting properties of TCP-1 fluorescence and radioligand with and without PEGylation, [ $^{99m}\text{Tc}$ ]Tc-HYNIC-PEG<sub>4</sub>-TCP-1 vs. [ $^{99m}\text{Tc}$ ]Tc-HYNIC-TCP-1.

**Results:** Fluorescence images showed that TCP-1 probes were distributed in the cytoplasm and nucleus of CRC cells. When CT26 cells were treated with unlabeled TCP-1 peptide prior to the cell incubation with Cy7-PEG<sub>4</sub>-TCP-1, cell fluorescent signals were significantly reduced relative to the cells without blockade. Relative to Cy7-TCP-1, superior brilliance and visibility of fluorescence was observed in the tumor with Cy7-PEG<sub>4</sub>-TCP-1 and maintained up to 18 hours post-injection. [ $^{99m}\text{Tc}$ ]Tc-HYNIC-PEG<sub>4</sub>-TCP-1 images in xenografted and orthotopic CRC models demonstrated that TCP-1 PEGylation preserved tumor targeting capability of TCP-1, but its distribution (%ID/g) in the liver and intestine was higher than that of [ $^{99m}\text{Tc}$ ]Tc-HYNIC-TCP-1 ( $1.51 \pm 0.29$  vs  $0.53 \pm 0.12$ ,  $P < 0.01$ ). Better tumor visualization by [ $^{99m}\text{Tc}$ ]Tc-HYNIC-TCP-1 was observed in the orthotopic CRC model due to lower intestinal radioactivity.

**Conclusions:** TCP-1-based probes undergo endocytosis and localize in the cytoplasm and nucleus of human and mouse CRC cells. Tumor detectability of fluorescent TCP-1 peptide with a PEG<sub>4</sub>

spacer is promising due to its enhanced tumor binding affinity and rapid clearance kinetics from nontumor tissues. Non-PEGylated [ $^{99m}\text{Tc}$ ]Tc-HYNIC-TCP-1 exhibits lower nonspecific accumulation in the liver and gastrointestinal tract and might have better capability for detecting CRC lesions in clinical sites. TCP-1 may represent an innovative targeting molecule for detecting CRC noninvasively.

**KEYWORDS:** Colorectal cancer; molecular imaging; fluorescence;  $^{99m}\text{Tc}$ ; TCP-1 peptide.

## Introduction

c[Cys-Thr-Pro-Ser-Pro-Phe-Ser-His-Cys]OH (TCP-1) is a small cyclic peptide identified by phage display selection from orthotopic mouse colorectal cancer (CRC). Previous data demonstrated that TCP-1 can recognize mouse and human CRC lesions and distinguish pre-malignant or early malignant colon lesions from non-tumor inflammatory tissues [1-5]. CRC is often caused by chronic inflammation of the intestinal mucosa rather than by any definitive genetic predisposition [6]. Differentiation of malignant lesions from inflammatory colorectal tissues is critically important and challenging in clinical practice [7]. A specific imaging technique for detection of CRC that will recognize early malignant transformation in asymptomatic patients or individuals who are susceptible to cancerous tissues is an unmet need [8,9]. TCP-1 holds potential as a molecular imaging probe with unique properties for early CRC detection. Evidence collected in mouse models with early cancer indicates that TCP-1 is capable of discriminating CRC from normal or inflamed colorectal tissues. Moreover, TCP-1 binding occurs in CRC cells and tumor vasculature, implying its involvement in tumor-associated angiogenesis. It is possible that TCP-1 homing to tumor is related to tumor-associated angiogenesis. Targeting of both cancer cells and tumor vasculature offers an advantage over those binding only cancer cells or vessels because of increased number of targets [2,10]. Furthermore, based on images acquired by TCP-1-conjugated quantum dots, TCP-1 may be a nuclear localization signal (NLS) peptide, in which a protein is tagged for import into the cell nucleus by nuclear transport [2,11,12]. Cell internalization and subcellular distribution of TCP-1 have not been defined to date in fluorescent or radiolabeled TCP-1 analogs.

Previously, we radiolabeled TCP-1 peptide with  $^{99m}\text{Tc}$  via 6-hydrazinopyridine-3-carboxylic acid (HYNIC) conjugation to produce [ $^{99m}\text{Tc}$ ]Tc-HYNIC-TCP-1 for imaging CRC [5]. Our *in vivo*

imaging data showed evidence that [ $^{99m}\text{Tc}$ ]Tc-HYNIC-TCP-1 could localize in human HCT116 CRC xenografts and spontaneous malignant lesions but did not home to xenografted prostate cancer sites. To further validate the ability of TCP-1 probes for targeting CRC and establish optimal probes for translatable imaging studies, we have synthesized PEGylated TCP-1 conjugates and labeled them with  $^{99m}\text{Tc}$  and near-infrared (NIR) dye, Cyanine7 (Cy7). The objectives of this study were to elucidate intracellular distribution of PEGylated and non-PEGylated TCP-1 probes in mouse and human CRC cells, determine their CRC-targeting specificity, and compare their feasibility for localizing CRC tissues in mouse models with xenografted and orthotopic tumors.

## **Materials and Methods**

### ***Peptide Conjugation***

The TCP-1 peptide was commercially synthesized at GL Biochem (Shanghai, China) according to our specifications. The TCP-1 peptides were prepared at purity > 95% at 254 nm by analytical high-performance liquid chromatography (HPLC).

**Synthesis of HYNIC-TCP-1 and HYNIC-PEG<sub>4</sub>-TCP-1.** N-hydroxysuccinimide ester of HYNIC (**1**) reacted with the terminal amino group of TCP-1 to produce HYNIC-TCP-1 (**2**) in the presence of 1-hydroxy-7-azabenzotriazole (HOAt) to accelerate the reaction. HYNIC-PEG<sub>4</sub>-TCP-1 (**4**) was prepared by reacting (**1**) first with amino-dPEG<sub>4</sub>-acid (Quanta BioDesign, Ltd., Plain City, Ohio) to provide an intermediate (**3**) which was subsequently coupled with TCP-1 using the peptide coupling reagent, N,N,N',N'-tetramethyl-O-(1H-benzotriazol-1-yl)uranium hexafluorophosphate (HBTU). The chemical structures of the PEGylated and non-PEGylated TCP-1 conjugates are shown in **Fig 1**.

**Cy7-TCP-1 (6)** was prepared by coupling the terminal amino group of TCP-1 with the Cy7

carboxylic salt (**5**) in the presence of HBTU. **Cy7- PEG4-TCP-1 (8)** was prepared by coupling amino-dPEG4-t-butyl ester with (**5**) to provide an intermediate which was purified by column chromatography and subsequently treated with 75%TFA to provide carboxylic acid (**7**). TCP-1 and (**7**) were coupled together using HBTU.

Detailed synthetic procedures and characterizations of PEGylated and non-PEGylated TCP-1 conjugates are presented in Electronic Supplementary Material (ESM) (see **Fig. S1-S6**).

### ***Radiolabeling TCP-1 with <sup>99m</sup>Tc***

Radiolabeling took place by adding pertechnetate (<sup>99m</sup>TcO<sub>4</sub><sup>-</sup>) in saline (370-555 MBq, 0.5 mL) to the vial containing 15 µg of HYNIC-TCP-1 or HYNIC-PEG4-TCP-1, 30 mg of tricine, 10 mg of EDDA, and 15 µg of tin chloride dihydrate and incubating the mixture for 30 minutes at 80°C. After HPLC purification, radiochemical purity (RCP) was greater than 99% for animal administration within 1 hour. Details of radiolabeling TCP-1 conjugates with <sup>99m</sup>Tc can be found in ESM.

### ***Stability test of the radiolabeled peptides***

*In vitro* stability of the radiolabeled peptides was tested by incubating 37 MBq of the radiolabeled product in mouse serum and saline (0.4 mL) at 37°C for 1 and 6 hours, respectively. Subsequently, the samples were centrifuged (4000 g, 4 °C) for 5 minutes, and 25 µL aliquots of the supernatant were analyzed by RP-HPLC [13].

### ***CRC cell lines***

CT26 mouse CRC cell line, human HCT116, HCT116/RFP, and HT29 CRC cell lines were obtained from the American Type Culture Collection (ATCC) (Rockville, MD). Cells were

cultured in RPMI and McCoy's 5a Medium and supplemented with 10% (v/v) fetal bovine serum (FBS), 100 U/mL penicillin, and 100 µg/mL streptomycin respectively (5% CO<sub>2</sub>, 37 °C).

### ***Cell imaging with fluorescent TCP-1 peptides***

Cancer cell lines were plated on coverslips by adding 500 µL of culture media containing approximately 5000 cells to the 6-well cell culture plate containing gelatin-coated coverslips. The cells were incubated overnight to promote adherence. Cy7-TCP-1 and Cy7-PEG<sub>4</sub>-TCP-1 probes (final concentration, 0.3 µM) were added in duplicate wells of each cell line, respectively, and incubated for 1 h at 37°C.

Cy7-PEG<sub>4</sub>-TCP-1 cell binding specificity was assessed using the CT26 cell line in a competitive binding assay. Cells were pretreated with 100 nM unconjugated TCP-1 (10 µM final concentration in the culture medium) twenty minutes prior to the addition of Cy7-PEG<sub>4</sub>-TCP-1. After incubation for 20 minutes, the cells were washed three times with ice-cold binding buffer before Cy7-PEG<sub>4</sub>-TCP-1 was loaded.

To verify subcellular localization of Cy7-TCP-1, Cy5.5-labeled hyaluronic acid (HA) with a molecular weight of 10 kDa (Cy5.5-HA) was incubated with HCT29 cells to illustrate appearance of the cytoplasm and nucleus of cancerous cells. Cy5.5-HA 10 µL was added to the well containing about 5000 cells and incubated for 2 hours.

After incubation with the fluorescent agents, cells on the coverslips were washed twice with PBS and incubated in a solution of formalin for 15-min fixation and then counterstained with 4',6-diamidino-2-phenylindole (DAPI) for 10 minutes at room temperature to visualize the cell nuclei. After a final rinse with PBS, the coverslips were mounted for microscopic examination using a Nikon E600 microscope (Nikon Instruments Inc., Melville, NY) with an ICG filter.

### ***Establishment of mouse CRC models***

Athymic nude mice and severe combined immunodeficient (SCID) mice weighing 18-22 g were obtained from the Experimental Mouse Shared Resource at the University of Arizona Comprehensive Cancer Center to establish CRC models for *in vivo* imaging studies with TCP-1 probes. HCT116 and CT26 cell lines were used to establish CRC models by subcutaneously injecting  $9 \times 10^6$  cancer cells into the nude mouse right shoulder. These models were adopted to define the targeting properties of TCP-1 probes to CRC tissues of human and murine origin. After 7 to 10 days when tumors reached 5-15 mm in diameter, the mice were recruited to start imaging studies for 2-3 times with  $^{99m}\text{Tc}$ -labeled TCP-1 probes.

An orthotopic CRC model was prepared by cecal implantation of HCT116 cancer cells in 10 SCID mice using a surgical procedure [14]. Under anesthesia with 1.0-1.5% isoflurane, a 0.5-inch long midline skin incision was made along the lower abdomen.  $0.5\text{-}1.0 \times 10^7$  CRC cells in 50  $\mu\text{l}$  PBS were injected into the cecal wall. The abdominal muscle layer was sutured and followed by skin closure using wound clips.

### ***In vivo imaging of mice with CRC***

Images of [ $^{99m}\text{Tc}$ ]Tc-HYNIC-TCP-1 and [ $^{99m}\text{Tc}$ ]Tc-HYNIC-PEG<sub>4</sub>-TCP-1 in CRC mouse models were acquired using a novel Quantum Imaging Detector (iQID) camera developed at University of Arizona [15-17]. HCT116 xenografts were imaged with [ $^{99m}\text{Tc}$ ]Tc-HYNIC-TCP-1 (n=6) and [ $^{99m}\text{Tc}$ ]Tc-HYNIC-PEG<sub>4</sub>-TCP-1 (n=7), respectively. Five survival mice bearing orthotopic HCT116 tumors were also imaged with [ $^{99m}\text{Tc}$ ]Tc-HYNIC-TCP-1 (n=2) and [ $^{99m}\text{Tc}$ ]Tc-HYNIC-PEG<sub>4</sub>-TCP-1 (n=3). Approximately 1.0  $\mu\text{g}$  [ $^{99m}\text{Tc}$ ]Tc-labeled TCP-1 peptide (~37 MBq, 0.2 mL) was given by direct tail-vein injection to the mice. Anesthetized mice were imaged 2-3 times within

4 hours using 15-min image acquisition. Planar images were produced using AMIDE 1.0.4 software.

Five animals bearing HCT116/RFP xenografts among the 13 mice above were intravenously injected with 25  $\mu\text{g}$  Cy7-TCP-1 (n=2) and Cy7-PEG<sub>4</sub>-TCP-1 (n=3) at 24 hours before administration of [<sup>99m</sup>Tc]Tc-HYNIC-TCP-1 or [<sup>99m</sup>Tc]Tc-HYNIC-PEG<sub>4</sub>-TCP-1, respectively, and imaged using Lago Optical Imaging System (Spectral Instruments, Tucson, AZ) with an ICG filter for acquiring *in vivo* Cy7 (excitation wavelength 745 nm and emission wavelength 810 nm) and RFP signals (excitation: 680/30 nm; emission: 775/30 nm). All fluorescence images were acquired and analyzed using the AMIView software of Spectral Instruments.

To define the targeting properties of TCP-1 in murine CRC cells, [<sup>99m</sup>Tc]Tc-HYNIC-PEG<sub>4</sub>-TCP-1 was intravenously administered in 10 mice bearing CT26 xenografts. Five mice were used for blocking tests by intravenous injection of 100  $\mu\text{g}$  non-radiolabeled TCP-1 at 10-min before [<sup>99m</sup>Tc]Tc-HYNIC-PEG<sub>4</sub>-TCP-1 administration. The other five mice received saline as carrier vehicle control. These mice were imaged using same procedures as performed in the mice with HCT116 tumors.

### ***Postmortem assays***

All mice were sacrificed at the end of the imaging session, and samples of tumor, blood, kidney, liver, heart, lung and skeletal muscle were harvested. The tissue samples were weighed, and the radioactivity was measured to calculate the percentage of injected dose per gram of tissue (%ID/g). The tumors were excised and fixed in formalin-saline for 24 hours and then paraffin-embedded for future use.

### *Statistical analysis*

All quantitative results were expressed as mean  $\pm$  S.E.M. Comparisons between two variables were performed with one-way analysis of variance. Probability values less than 0.05 were considered significant.

## **Results**

### *Production and Characterization of HYNIC-TCP-1 and HYNIC-PEG<sub>4</sub>-TCP-1*

As shown in ESM **Fig. S3**, the analytical HPLC profile of HYNIC-TCP-1 showed two peaks at 22.2 min and 24.6 min corresponding to HYNIC-TCP-1 minus the acetone hydrazone protecting group and HYNIC-TCP-1 respectively. Two peaks at 19.3 min and 20.1 min correspond to the product of HYNIC-PEG<sub>4</sub>-TCP-1 with and without the acetone protecting group respectively (see **Fig. S3**). In comparison to the HYNIC-TCP-1, incorporation of the PEG<sub>4</sub> spacer enhanced the hydrophilicity of the HYNIC-PEG<sub>4</sub>-TCP-1 conjugate as evidenced by a shorter retention time on HPLC.

### *Production and Characteristics of Cy7-TCP-1 and Cy7-PEG<sub>4</sub>-TCP-1*

The mass spectrum of Cy7-TCP-1 demonstrated a peak for the expected parent  $M+H = 1846.7$  and for  $(M+Na)^+ = 1869$ . In contrast, Cy7-PEG<sub>4</sub>-TCP-1 mass spectrum exhibited the expected parent  $M+H = 2094.1$  mass units ( see **Fig. S5**). The analytical HPLC profiles of Cy7-TCP-1 and Cy7-PEG<sub>4</sub>-TCP-1 showed a main peak at 794 nm with retention time of 25.5 min for both and purity of 86% and 98.6%, as shown in **Fig. S6**.

### *Radiolabeling yield and stability*

The labeling yield of the product was 92-95% and the radiochemical purity was greater than 99% after HPLC purification. After 1-h and 6-h of incubation at 37°C, more than 98% and 95% of <sup>99m</sup>Tc-labeled TCP-1, respectively, remained intact in saline or mouse serum as shown in **Fig. S7**. There was no evidence of any metabolism occurring in serum.

### ***In vitro cell uptake of Cy7-TCP-1 and Cy7-PEG<sub>4</sub>-TCP-1***

After 60-min incubation, prominent fluorescence signal of PEGylated and non-PEGylated Cy7-TCP-1 conjugates in CRC cells was observed by fluorescence microscopy. As shown in **Fig. 2a** and **2b**, cell uptake intensity of Cy7-PEG<sub>4</sub>-TCP-1 was equivalent to that of Cy7-TCP-1 when the CT26 cells were incubated and imaged under the same conditions. The signal intensity measured in arbitrary units and corrected by subtracting background signal was  $30.8 \pm 2.2$  vs.  $31.9 \pm 2.3$  for PEGylated and non-PEGylated TCP-1 ( $P > 0.05$ ). We examined the cell binding specificity of Cy7-PEG<sub>4</sub>-TCP-1 using a blocking study in CT26 cell line. As demonstrated in **Fig. 2c** and **2d**, prominent fluorescence signal was observed for cells stained with fluorescence in the absence of TCP-1 blockade. Cell-associated fluorescence intensity was decreased when the cells were pretreated with a blocking dose of unlabeled TCP-1 ( $26.3 \pm 2.0$  vs.  $8.1 \pm 0.6$ ,  $P < 0.01$ ). Based on the fluorescence distribution, Cy7-TCP-1 and Cy7-PEG<sub>4</sub>-TCP-1 appeared in the cytoplasm and cell nuclei. In contrast, nonspecific Cy5.5-HA, which was used to illustrate the cytoplasmic appearance, was internalized and distributed only in the cytoplasm in the same cell line. Representative fluorescence images of Cy7-TCP-1 and Cy5.5-HA in the HT29 cells are presented in **Fig. 3**.

### ***In vivo imaging of CRC tumor models***

***In vivo NIR fluorescence imaging.*** Fifteen minutes post administration of Cy7-TCP-1 and Cy7-

PEG<sub>4</sub>-TCP-1, the fluorescent signal was detected from the whole mouse body. Subsequently, fluorescence was rapidly eliminated from the nontumor tissues. At 15-30 minutes, tumor xenografts in the mice started to show focal uptake of fluorescence. Cy7-PEG<sub>4</sub>-TCP-1 showed 1.3-fold greater brilliance and visibility of fluorescence in the tumors than Cy7-TCP-1. The fluorescence of Cy7-PEG<sub>4</sub>-TCP-1 in the xenografted tumor became clearly detectable at 30 minutes and remained prominent up to 18 hours at the end of imaging session, as shown in **Fig. 4**. Using RFP optical images as a map, tumor sites and fluorescence uptake levels were readily assessable. Moderate fluorescent signal was observed from the ventral view over the abdominal area of the mice injected with Cy7-PEG<sub>4</sub>-TCP-1, as shown in **Fig. 4e**. The signal intensity of tumor tissues was consistently higher than that in the abdomen.

**iQID imaging of [<sup>99m</sup>Tc]Tc-HYNIC-TCP-1 and [<sup>99m</sup>Tc]Tc-HYNIC-PEG<sub>4</sub>-TCP-1.** Whole-body iQID imaging depicted overall biodistributions of <sup>99m</sup>Tc-labeled TCP-1 probes in the mice with xenografted HCT116 tumors. **Fig. 5** shows representative [<sup>99m</sup>Tc]Tc-HYNIC-PEG<sub>4</sub>-TCP-1 and [<sup>99m</sup>Tc]Tc-HYNIC-TCP-1 images in mice with large-sized and medium-sized HCT116 xenografts. Typically, the tumor lesions became detectable at early stages around 5-7 days after tumor implantation. Afterwards, radioactive uptake in the tumor was increased along with tumor growth. The xenografted HCT116 tumors were readily detectable at 10-14 days. Quantitatively, the tumor uptake of [<sup>99m</sup>Tc]Tc-HYNIC-PEG<sub>4</sub>-TCP-1 and [<sup>99m</sup>Tc]Tc-HYNIC-TCP-1 was identical in the HCT116 xenografts. The ratio of tumor-to-nontumor radioactivity determined by region-of-interest (ROI) analysis over the tumor and left shoulder or neck area was  $2.38 \pm 0.18$  (n=6) and  $2.14 \pm 0.20$  (n=7), respectively, ( $P > 0.05$ ). Based on SPECT imaging data in our previous studies and postmortem analyses in this study, radioactive distribution of [<sup>99m</sup>Tc]Tc-HYNIC-TCP-1 and [<sup>99m</sup>Tc]Tc-HYNIC-PEG<sub>4</sub>-TCP-1 was prominently associated with rapidly growing tumor tissues

with lack of uptake in necrotic tumor areas. As illustrated in **Fig. 5**, significantly higher radioactive accumulation appeared in the liver and intestines on images of [<sup>99m</sup>Tc]Tc-HYNIC-PEG<sub>4</sub>-TCP-1. [<sup>99m</sup>Tc]Tc-HYNIC-TCP-1 excretory activity was prominent in the kidneys and bladder, less in the liver and intestines.

When [<sup>99m</sup>Tc]Tc-HYNIC-PEG<sub>4</sub>-TCP-1 was administered to animals bearing CT26 mouse CRC (n=5), the radioactive levels of the tumor masses were similar to the radioactive uptake of HCT116 tumors. When mice were pretreated with unlabeled TCP-1 peptide prior to [<sup>99m</sup>Tc]Tc-HYNIC-PEG<sub>4</sub>-TCP-1 administration, radioactivity in the tumors (n=5) was significantly reduced as shown in **Fig. 6**. The ratio of tumor-to-nontumor radioactivity in CT26 tumor without and with blockade was 2.33±0.24 vs. 1.35±0.08 ( $P < 0.05$ ).

Among ten mice recruited to establish the orthotopic HCT116 tumor model, five were survived and developed cecal tumors during the 20 weeks after cancer cell implantation. As shown in **Fig. 7**, iQID images with [<sup>99m</sup>Tc]Tc-HYNIC-TCP-1 and [<sup>99m</sup>Tc]Tc-HYNIC-PEG<sub>4</sub>-TCP-1 in the orthotopic tumors of the same cell line and similar localization showed comparable radioactive uptake in the time window of 30-240 minutes post tracer injection. The average ratio of tumor-to-nontumor radioactivity in the five mice was 2.18±0.35. In mice injected with [<sup>99m</sup>Tc]Tc-HYNIC-PEG<sub>4</sub>-TCP-1, moderate levels of radioactive accumulation in the intestinal regions presumably resulted from hepatobiliary excretion. Lower accumulation of [<sup>99m</sup>Tc]Tc-HYNIC-TCP-1 in the intestinal tract made abdominal tumors more apparent than on [<sup>99m</sup>Tc]Tc-HYNIC-PEG<sub>4</sub>-TCP-1 images.

### ***Biodistribution measurements***

Postmortem biodistribution measurements (%ID/g) in the mice bearing xenografted tumors are summarized in **Table 1**. [ $^{99m}\text{Tc}$ ]Tc-HYNIC-TCP-1 showed prominent renal excretion and low uptake in the liver and gut. The HCT116 tumors accumulated significantly higher radioactivity of [ $^{99m}\text{Tc}$ ]Tc-HYNIC-TCP-1 than blood, muscle, and skin ( $P < 0.001$ ). Similarly, HCT116 tumors in the mice receiving [ $^{99m}\text{Tc}$ ]Tc-HYNIC-PEG<sub>4</sub>-TCP-1 showed higher radioactive uptake than the soft tissues, but liver uptake in these animals was higher than that in the mice receiving [ $^{99m}\text{Tc}$ ]Tc-HYNIC-TCP-1. Uptake of [ $^{99m}\text{Tc}$ ]Tc-HYNIC-PEG<sub>4</sub>-TCP-1 in the CT26 tumor xenografts was not significantly different compared to that in the HCT116 tumors. When unlabeled TCP-1 was administered prior to [ $^{99m}\text{Tc}$ ]Tc-HYNIC-PEG<sub>4</sub>-TCP-1, radioactive uptake in the CT26 tumors was reduced significantly ( $P < 0.05$ ).

## Discussion

CRC diagnostic methods have lacked practical molecular imaging probes [18-20]. Key issues in synthesizing CRC-targeting molecular imaging probes are high binding specificity, sensitivity, and affinity to tumor cells, and low normal gastrointestinal activity. Since different  $^{99m}\text{Tc}$  chelators as well as linking groups can affect the overall hydrophilicity and charge of the tracer and can therefore affect biodistribution and tumor uptake properties, we have designed probes in which linking group parameters are varied to establish the optimal analogues for imaging studies. Accordingly, we have synthesized HYNIC-PEG<sub>4</sub>-TCP-1 and Cy7-PEG<sub>4</sub>-TCP-1 and performed comparison studies with non-PEGylated versions to optimize TCP-1 analogues with high selectivity for CRC targeting and low nonspecific radioactive accumulation in the gastrointestinal tract.

Previous reports described the specificity of TCP-1 analogues in murine and human CRC

lesions [1,2]. The results in this study provide further evidence of TCP-1 specific binding to murine colon carcinoma. [<sup>99m</sup>Tc]Tc-HYNIC-PEG<sub>4</sub>-TCP-1 *in vivo* blocking test showed selectivity for mouse CRC. [<sup>99m</sup>Tc]Tc-HYNIC-PEG<sub>4</sub>-TCP-1 tumor uptake in animals receiving unlabeled TCP-1 was significantly reduced, consistent with results of human CRC cells in a previous report [1]. Currently, the specific target for TCP-1 has not been elucidated. The receptors may be unique to neoplastic cells in CRC, or they may be expressed at low levels in healthy tissues but elevated in malignant tissues [2,10,21]. It is also possible that CRC cells and tumor-associated/derived endothelial cells share TCP-1 receptors [22,23]. CRC cells and tumor-associated endothelial cells express distinct molecules that do not exist in normal blood vessels or tissues [2,10]. Based on currently available data, it is reasonable to expect that TCP-1 molecular imaging should be able to localize human CRC by targeting both tumor cells and tumor-associated vasculature.

Kidney-mediated clearance is the major contributor to the fast clearance of non-PEGylated [<sup>99m</sup>Tc]Tc-HYNIC-TCP1, probably by glomerular filtration that sieves small molecules based on molecular size and electric charge of the substances. PEGylation of surface lysine residues is an effective means to improve the pharmacokinetic behavior and bioavailability of molecular imaging probes by increasing the molecular mass of peptides, shielding them from proteolytic enzymes, prolonging *in vivo* circulating half-lives, and lowering clearance. The chemical modification with PEG may allow parenteral peptides to avoid first-pass renal clearance, or other metabolic pathways, and extend their half-life in circulation [24]. Importantly, PEGylation may preserve the binding or function of a biomolecule. Our *in vitro* and *in vivo* data demonstrated that PEGylated TCP-1 retained its *in vivo* stability and tumor targeting properties as exhibited in the mouse model with heterotopic CRC transplant. Furthermore, the results of iQID imaging in the orthotopic CRC model, which resembles the original tumor microenvironment more closely, provided convincing

evidence that [ $^{99m}\text{Tc}$ ]Tc-HYNIC-PEG<sub>4</sub>-TCP-1 preserved the tumor targeting properties of TCP-1. Compared to [ $^{99m}\text{Tc}$ ]Tc-HYNIC-TCP-1 biodistribution, higher accumulation of [ $^{99m}\text{Tc}$ ]Tc-HYNIC-PEG<sub>4</sub>-TCP-1 was observed in the liver and intestines in this study, indicating that the catabolism of PEGylated TCP-1 might shift from kidney to liver, probably due to the increase in both molecular weight and hydrodynamic radius [25]. The resulting hepatobiliary excretion and increased intestinal radioactivity of [ $^{99m}\text{Tc}$ ]Tc-HYNIC-PEG<sub>4</sub>-TCP-1 may interfere with observation of abdominal and pelvic tumors by gamma-ray imaging. Unlike [ $^{99m}\text{Tc}$ ]Tc-HYNIC-PEG<sub>4</sub>-TCP-1, [ $^{99m}\text{Tc}$ ]Tc-HYNIC-TCP-1 showed less radioactive accumulation in the liver and intestines. Acceptable target-to-nontarget ratios may be reached for tumor detection at 30-120 minutes after tracer injection. Although significantly higher radioactive accumulation may occur in the bladder, emptying the bladder prior to image acquisition may mitigate the drawback of urinary excretion. Thus, [ $^{99m}\text{Tc}$ ]Tc-HYNIC-TCP-1 imaging may provide a complementary method to colonoscopy for differential diagnosis of indeterminate lesions, thereby improving patient outcomes.

NIR imaging of CRC with TCP-1 fluorescence has shown promising results in this study. Due to advances in reduced autofluorescence, low photon scattering in biological tissues, and significantly less attenuation of light in the region (650–900 nm) compared with visible wavelengths, NIR fluorescence affords high spatial resolution and deeper tissue penetration. In mice with CRC xenografts, our NIR imaging revealed the unique capability of Cy7-PEG<sub>4</sub>-TCP-1 in tumor visualization and long-lasting tumor retention. The persistently retained feature of Cy7-TCP-1 in the CRC tissues may result from its cellular internalization, subcellular translocation, and nuclear localization. Our *in vitro* cell studies showed that the fluorescence probes of TCP-1 underwent endocytosis and distributed in the cytoplasm and nucleus [1,2]. In contrast, cell culture

studies with Cy5.5-HA, in which HA can distribute in the cytoplasm but not in the nucleus, showed absence of fluorescence in the nuclei of CRC cells. It is speculated that TCP-1 is a nuclear localization signal (NLS) peptide, which acts as a signal fragment for direct import of proteins into the cell nucleus from the cytoplasm by nuclear transport [11,12].

Cy7-PEG<sub>4</sub>-TCP-1 exhibited high and selective uptake in the xenografted tumors with long-lasting visibility up to 18 hours. Our *in vitro* and *in vivo* data support the potential of Cy7-PEG<sub>4</sub>-TCP-1 for clinical application in fluorescence endoscopy, particularly in the setting of inflammatory bowel disease (IBD). Nonspecific accumulation of dyes or imaging agents in inflammatory tissue may result in false-positive results for malignant lesion detection in an inflammatory site [7]. TCP-1 peptide may have fundamentally distinct targeting capability with selectivity for CRC within the inflammatory colorectal microenvironment. Endoscopic methods such as fluorescence-guided or confocal endoscopy may be used to identify fluorescent TCP-1 and accurately localize biopsy sites having a high contrast tumor lesion with low background.

There are some limitations in this study. We did not include a negative control peptide labeled with Cy7 for preclinical experiments. Previously, our results with the inactive peptide, [<sup>99m</sup>Tc]Tc-HYNIC-CVQTAQLLC, supported specificity of [<sup>99m</sup>Tc]Tc-HYNIC-TCP-1 in the HCT116 xenografts. The tumor xenografts showed only slightly increased uptake of inactive peptide relative to muscle, probably caused by increased tumor vascular permeability. In addition, images of Cy7-TCP-1 and Cy7-PEG<sub>4</sub>-TCP-1 were only collected in a small number of mouse CRC models, not in the models with orthotopic CRC. A mouse model with spontaneous CRC in the inflammatory colorectal environment is required to further characterize the *in vivo* targeting properties of TCP-1 probes for detecting and discriminating early CRC lesions from inflammatory colonic sites by SPECT and fluorescence imaging.

## Conclusions

<sup>99m</sup>Tc- and Cy7-labeled TCP-1 peptides with and without PEGylation were characterized by *in vitro* and *in vivo* studies using CRC cells and murine tumor models. Two NIR fluorescent analogs, Cy7-TCP-1 and Cy7-PEG<sub>4</sub>-TCP-1 demonstrated their capabilities to provide a molecular signature in both human and mouse CRC cells. The TCP-1 probes were shown to specifically localize in the metabolically active cytoplasm and nucleus. *In vivo* optical imaging further delineated the feasibility of TCP-1-targeted detection of colorectal tumor xenografts with Cy7-TCP-1 and Cy7-PEG<sub>4</sub>-TCP-1. Using the planar iQID camera, *in vivo* imaging of [<sup>99m</sup>Tc]Tc-HYNIC-TCP-1 and [<sup>99m</sup>Tc]Tc-HYNIC-PEG<sub>4</sub>-TCP-1 demonstrated the uptake of TCP-1 probes in the CRC tissues including subcutaneous xenografts and orthotopic implantation of tumor in cecum.

The imaging results in living animals indicate that the PEGylation of TCP-1 probes could preserve the tumor targeting capability of TCP-1 peptide, but also enhance the hepatobiliary excretion of the TCP-1 radiolabeled probe, thereby interfering with visualization of tumor uptake by SPECT or planar gamma-camera imaging. In contrast, non-PEGylated [<sup>99m</sup>Tc]Tc-HYNIC-TCP-1 readily localized in CRC lesions and had low nonspecific accumulation in the gastrointestinal tract. The results in this study and our previous findings, in which uptake of the TCP-1 probe occurred in-metabolically active cancer lesions and tumor-associated vasculature, indicate that TCP-1 may represent an innovative targeting molecule for detecting CRC and its vasculature. Further studies of the mechanism of TCP-1 binding are warranted.

**Acknowledgments.** This study was funded by NIH grants NCI 1R21-CA216657, NIBIB P41-EB002035, and NCI P30-CA023074. The authors are grateful to Dr. Harrison Barrett, Director of the Center for Gamma-Ray Imaging, for making the facilities of the Center available for animal

imaging studies. We wish to thank Dr. Gail Stevenson for support in animal care. We are grateful to Drs. Arthur Gmitro and Andrew Rouse for their assistance in cell fluorescence imaging.

### ***Declarations***

**Conflict of Interest.** Drs. Koon Pak and Brian Gray are president and vice president for research of Molecular Targeting Technologies, Inc., respectively. Other authors declare that they have no conflict of interest.

**Ethics Approval.** All applicable institutional and/or national guidelines for the care and use of animals were followed. Animal protocols for cancer implantation and imaging studies were approved by the Institutional Animal Care and Use Committee (IACUC) at the University of Arizona.

### **References**

1. Li ZJ, Cho CH (2012) Peptides as targeting probes against tumor vasculature for diagnosis and drug delivery. *J Transl Med* 10 Suppl 1:S1.
2. Li ZJ, Wu WK, Ng SS, et al. (2010) A novel peptide specifically targeting the vasculature of orthotopic colorectal cancer for imaging detection and drug delivery. *J Control Release* 148(3):292-302.
3. Lu L, Li ZJ, Li LF, et al. (2015) Vascular-targeted TNFalpha improves tumor blood vessel function and enhances antitumor immunity and chemotherapy in colorectal cancer. *J Control Release* 210:134-46.
4. Shen J, Li ZJ, Li LF, et al. (2016) Vascular-targeted TNFalpha and IFNgamma inhibits orthotopic colorectal tumor growth. *J Transl Med* 14(1):187.

5. Liu Z, Gray BD, Barber C, Bernas M, Cai M, et al. (2016) Characterization of TCP-1 probes for molecular imaging of colon cancer. *J Control Release* 239:223-30.
6. Yang ZH, Dang YQ, Ji G (2019) Role of epigenetics in transformation of inflammation into colorectal cancer. *World J Gastroenterol* 25(23):2863-2877.
7. Cao Q, Liu S, Niu G, Chen K, Yan Y, Liu Z, Chen X (2011) Phage display peptide probes for imaging early response to bevacizumab treatment. *Amino Acids* 41(5):1103-12.
8. Enback J, Laakkonen P (2007) Tumour-homing peptides: tools for targeting, imaging and destruction. *Biochem Soc Trans* 35(Pt 4):780-3.
9. Laakkonen P, Vuorinen K (2010) Homing peptides as targeted delivery vehicles. *Integr Biol (Camb)* 2(7-8):326-37.
10. Laakkonen P, Zhang L, Ruoslahti E (2008) Peptide targeting of tumor lymph vessels. *Ann N Y Acad Sci* 1131:37-43.
11. Sturzu A, Regenbogen M, Klose U, et al. (2008) Novel dual labelled nucleus-directed conjugates containing correct and mutant nuclear localisation sequences. *Eur J Pharm Sci* 33(3):207-16.
12. Kalderon D, Roberts BL, Richardson WD, Smith AE (1984) A short amino acid sequence able to specify nuclear location. *Cell* 39(3 Pt 2):499-509.
13. Erfani M, Zarrabi Ahrabi N, Shafiei M, Shirmardi SP (2014) A (99m) Tc-tricine-HYNIC-labeled peptide targeting the neurotensin receptor for single-photon imaging in malignant tumors. *J Labelled Comp Radiopharm* 57(3):125-31.
14. Liao HW, Hung MC (2017) Intracaecal Orthotopic Colorectal Cancer Xenograft Mouse Model. *Bio Protoc* 7(11):e2311

15. Miller BW, Gregory SJ, Fuller ES, et al. (2014) The iQID camera: An ionizing-radiation quantum imaging detector. *Nucl Instrum Methods Phys Res A* 767:146-152.
16. Furenlid LR, Barrett HH, Barber HB, et al. (2014) Molecular Imaging in the College of Optical Sciences - An Overview of Two Decades of Instrumentation Development. *Proc SPIE Int Soc Opt Eng* 9186.
17. Han L, Miller BW, Barber HB, Nagarkar VV, Furenlid LR (2014) A New Columnar CsI(Tl) Scintillator for iQID detectors. *Proc SPIE Int Soc Opt Eng* 9214:92140D.
18. Schottelius M, Wester HJ (2009) Molecular imaging targeting peptide receptors. *Methods* 48(2):161-77.
19. Turker NS, Heidari P, Kucherlapati R, Kucherlapati M, Mahmood U (2014) An EGFR targeted PET imaging probe for the detection of colonic adenocarcinomas in the setting of colitis. *Theranostics* 4(9):893-903.
20. Kim J, Do EJ, Moinova H, et al. (2017) Molecular Imaging of Colorectal Tumors by Targeting Colon Cancer Secreted Protein-2 (CCSP-2). *Neoplasia* 19(10):805-816.
21. Oh P, Li Y, Yu J, et al. (2004) Subtractive proteomic mapping of the endothelial surface in lung and solid tumours for tissue-specific therapy. *Nature* 429(6992):629-35.
22. McGuire TF, Sajithlal GB, Lu J, Nicholls RD, Prochownik EV (2012) In vivo evolution of tumor-derived endothelial cells. *PLoS One* 7(5):e37138.
23. Meseure D, Drak Alsibai K, Nicolas A (2014) Pivotal role of pervasive neoplastic and stromal cells reprogramming in circulating tumor cells dissemination and metastatic colonization. *Cancer Microenviron* 7(3):95-115.

24. Turecek PL, Bossard MJ, Schoetens F, Ivens IA (2016) PEGylation of Biopharmaceuticals: A Review of Chemistry and Nonclinical Safety Information of Approved Drugs. *J Pharm Sci* 105(2):460-475.
25. Li Q, White JB, Peterson NC, et al. (2018) Tumor uptake of pegylated diabodies: Balancing systemic clearance and vascular transport. *J Control Release* 279:126-135.

## Figure Legends

**Fig. 1.** Chemical structures of the PEGylated and non-PEGylated TCP-1 conjugates, HYNIC-PEG<sub>4</sub>-TCP-1 and HYNIC-TCP-1.

**Fig. 2.** Microphotographs of TCP-1 fluorescence images (green) of CT26 mouse CRC cells (*Left column*), DAPI counter-stained nuclei (blue) (*Middle column*), and overlapped image (*Right column*). Fluorescence intensity was identical in the cell lines incubated with Cy7-TCP-1 (*a*) and Cy7-PEG<sub>4</sub>-TCP-1 (*b*). Fluorescence images (*c* and *d*) demonstrated that the treatment of CT26 CRC cells with TCP-1 blockade (*d*) prior to Cy7-PEG<sub>4</sub>-TCP-1 administration reduced the intensity of cell-associated TCP-1 fluorescence compared to the cells treated with PBS (*c*).

**Fig. 3.** Microphotographs of HT29 cells incubated in the media containing Cy7-TCP-1 (*a*) and Cy5.5-HA (*d*), DAPI counter-stained nuclei (*b* and *e*), and overlapped image (*c* and *f*). Merged Cy7-TCP-1 and DAPI images depicted nuclear and cytoplasmic localization of the TCP-1 fluorescence. The intracellular distribution of Cy5.5-HA fluorescence was observed in cytoplasm only.

**Fig. 4.** *In vivo* fluorescence images of two mice with subcutaneously located HCT116 tumors (indicated by arrows) with administration of Cy7-PEG<sub>4</sub>-TCP-1 (*b, d, e*) and Cy7-TCP-1 (*f*). Cy7-PEG<sub>4</sub>-TCP-1 images in *b* and *d* were acquired from dorsal view at 0.5-h and 18-h post-injection. Image in *e* was acquired from the ventral view after *d* to compare the fluorescence levels between the tumor uptake and abdominal accumulation. The RFP-expressing HCT116 xenografts were visualized using excitation 680/30 nm and emission 775/ 30 nm and presented in *a, c*, and *g*.

**Fig. 5.** *a* and *b*: Representative iQID image of [<sup>99m</sup>Tc]Tc-HYNIC-PEG<sub>4</sub>-TCP-1 at 4-h post-injection showing increased radioactive uptake in large HCT116 xenografts expanded into right

and left mouse shoulder (indicated by arrows) after 20 days of cell implantation. Predominant radioactive accumulation was visible in the liver, kidneys, and bladder. *c and d*: [<sup>99m</sup>Tc]Tc-HYNIC-TCP-1 image in a mouse bearing HCT116 xenograft (marked by dotted outline) on the right shoulder after 16 days of cell implantation. Readily detectable tumor uptake (arrows) was observed at 4-h post-injection of [<sup>99m</sup>Tc]Tc-HYNIC-TCP-1. Predominant radioactivity was visible in the kidneys and bladder.

**Fig. 6.:** iQID images of [<sup>99m</sup>Tc]Tc-HYNIC-PEG<sub>4</sub>-TCP-1 in two mice bearing subcutaneous CT26 tumors (arrows) without TCP-1 blockade (*a and b*) and with blockade in overdose (*c and d*), respectively. Significantly decreased uptake of [<sup>99m</sup>Tc]Tc-HYNIC-TCP-1 was observed in the tumor with blockade.

**Fig. 7.** Representative iQID [<sup>99m</sup>Tc]Tc-HYNIC-TCP-1 (*a*) and [<sup>99m</sup>Tc]Tc-HYNIC-PEG<sub>4</sub>-TCP-1 image (*c*) in two mice with orthotopic HCT116 CRC. Focal radioactive uptake (arrows) detected in the cecal areas was associated with tumors observed by postmortem examination (arrows) (*b and d*). Compared to [<sup>99m</sup>Tc]Tc-HYNIC-PEG<sub>4</sub>-TCP-1, lower radioactive accumulation in the intestinal region was observed on [<sup>99m</sup>Tc]Tc-HYNIC-TCP-1 image.

**Figure 1**

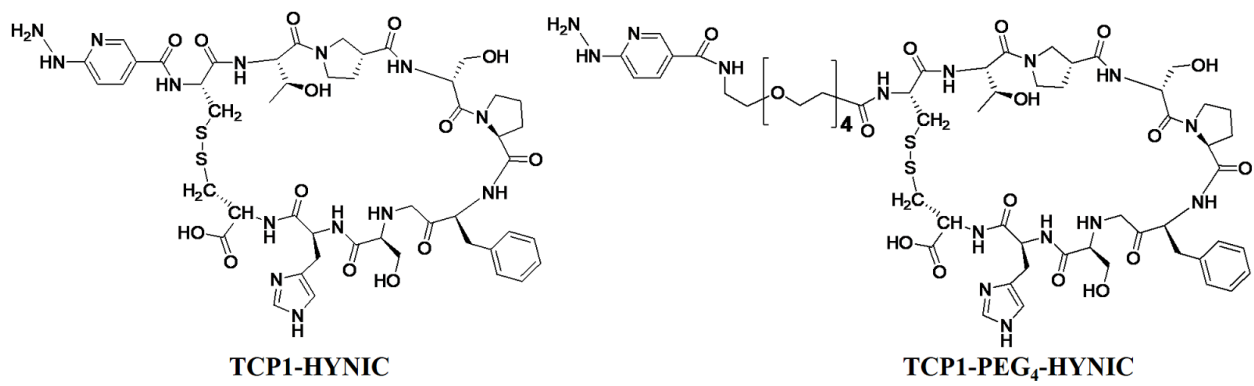


**Figure 2**

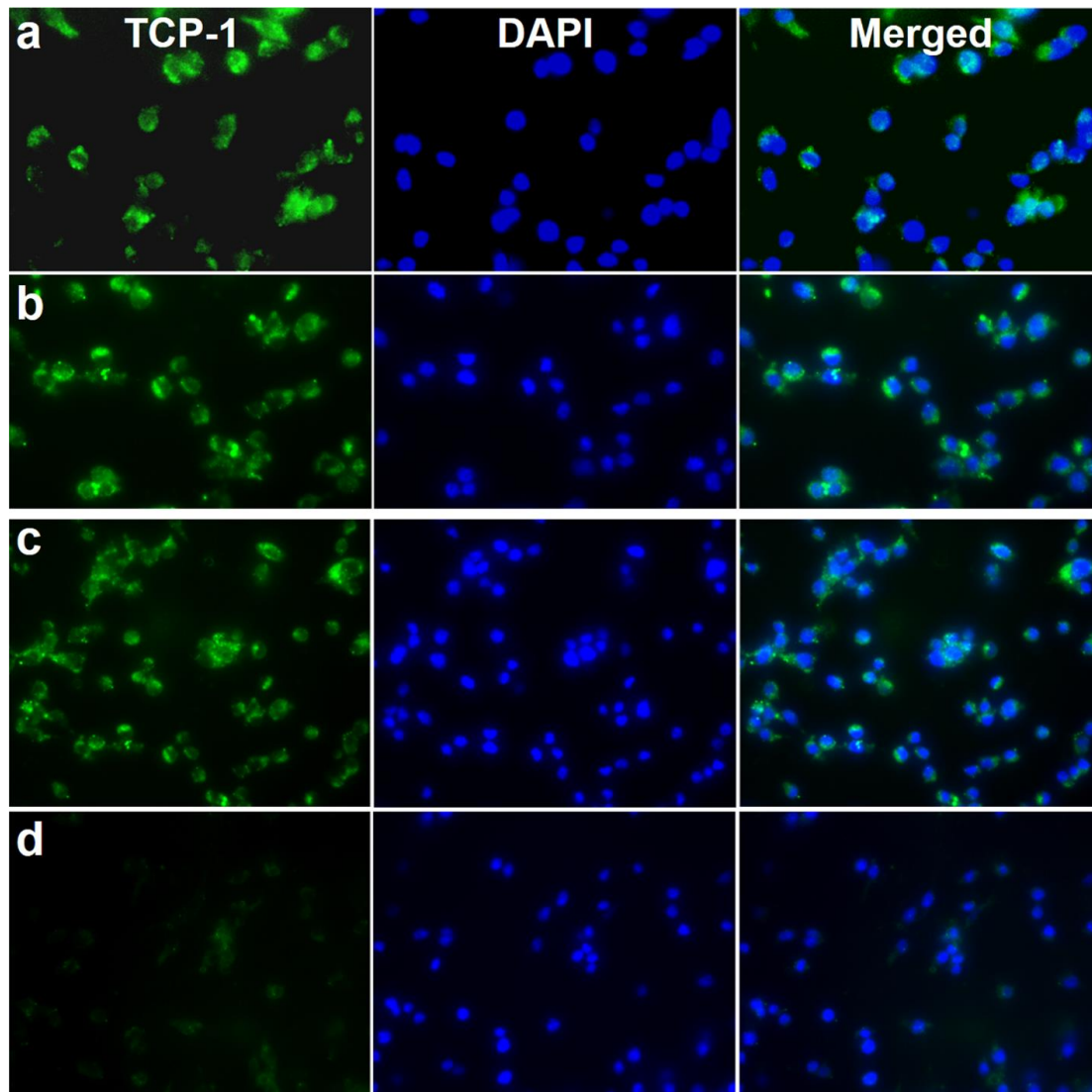


Figure 3

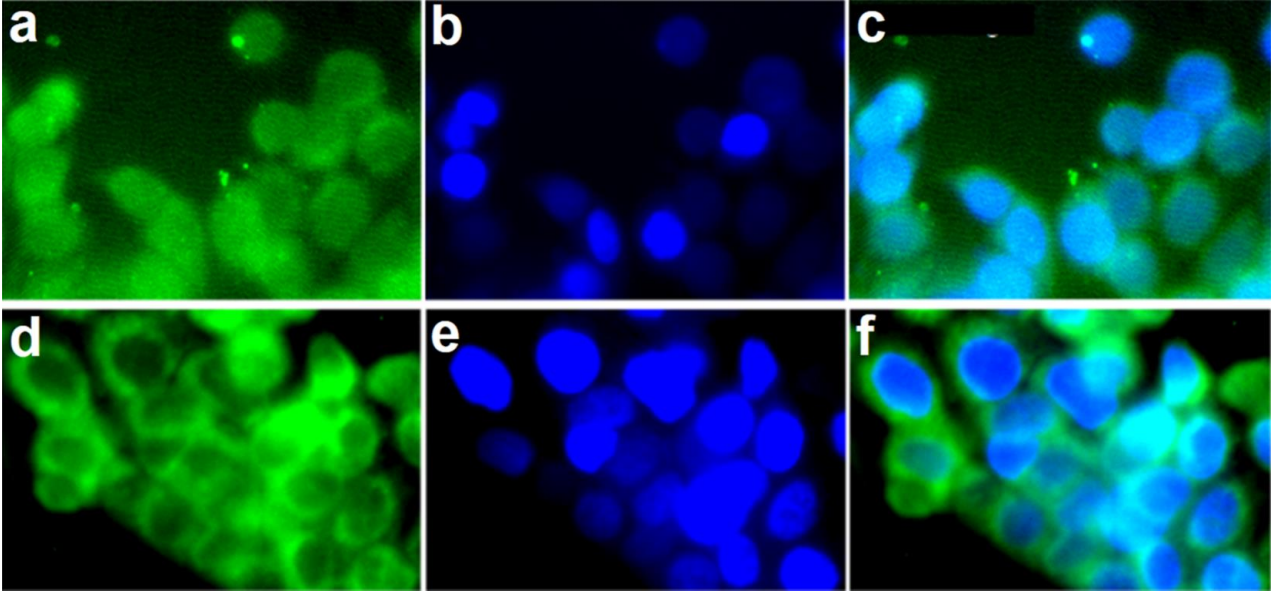


Figure 4

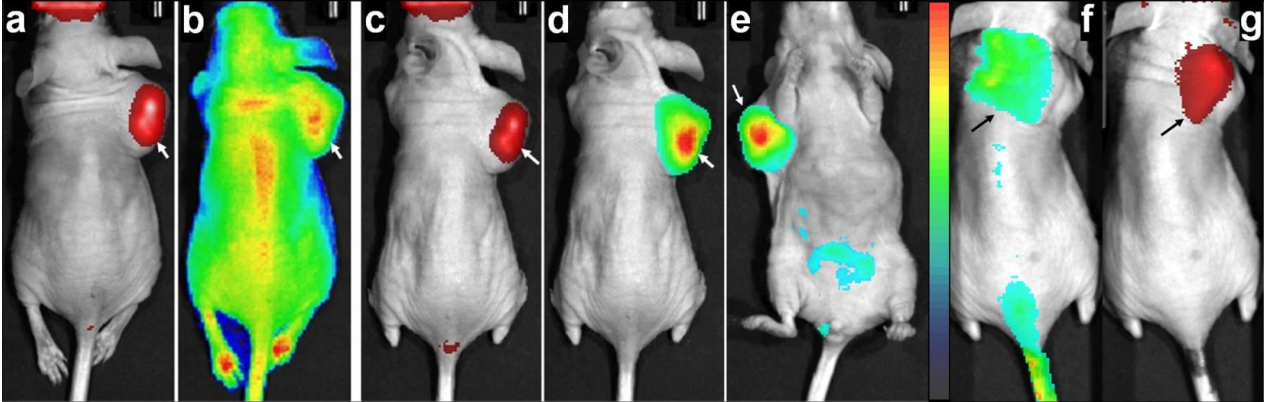


Figure 5

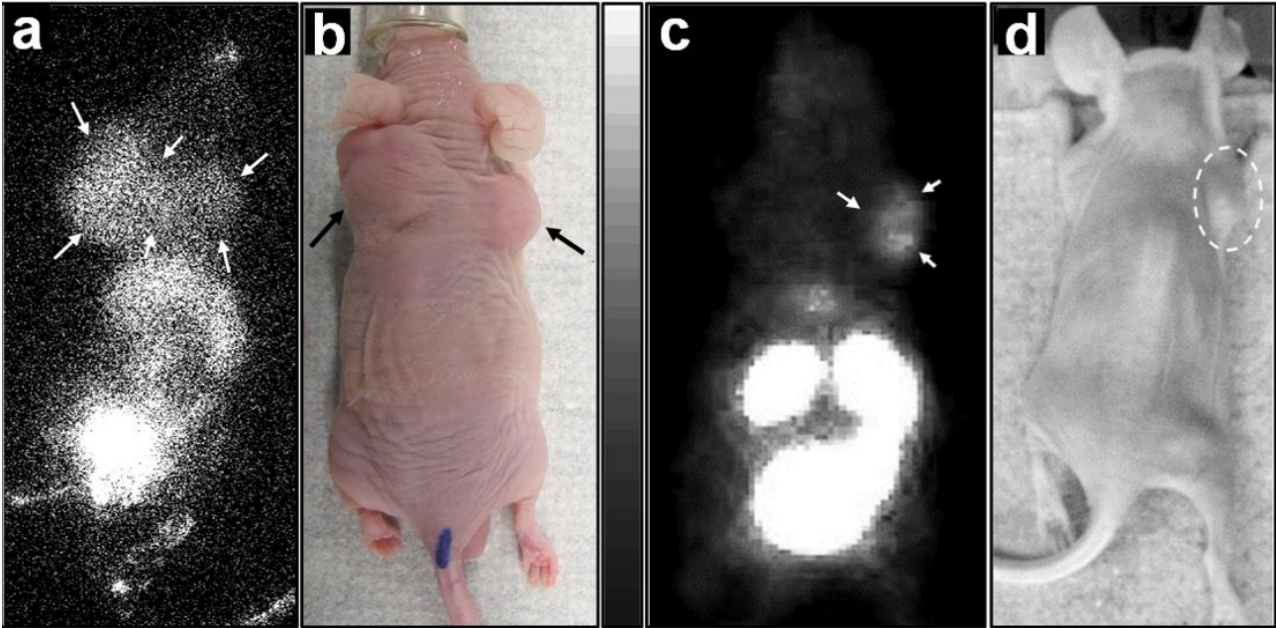


Figure 6

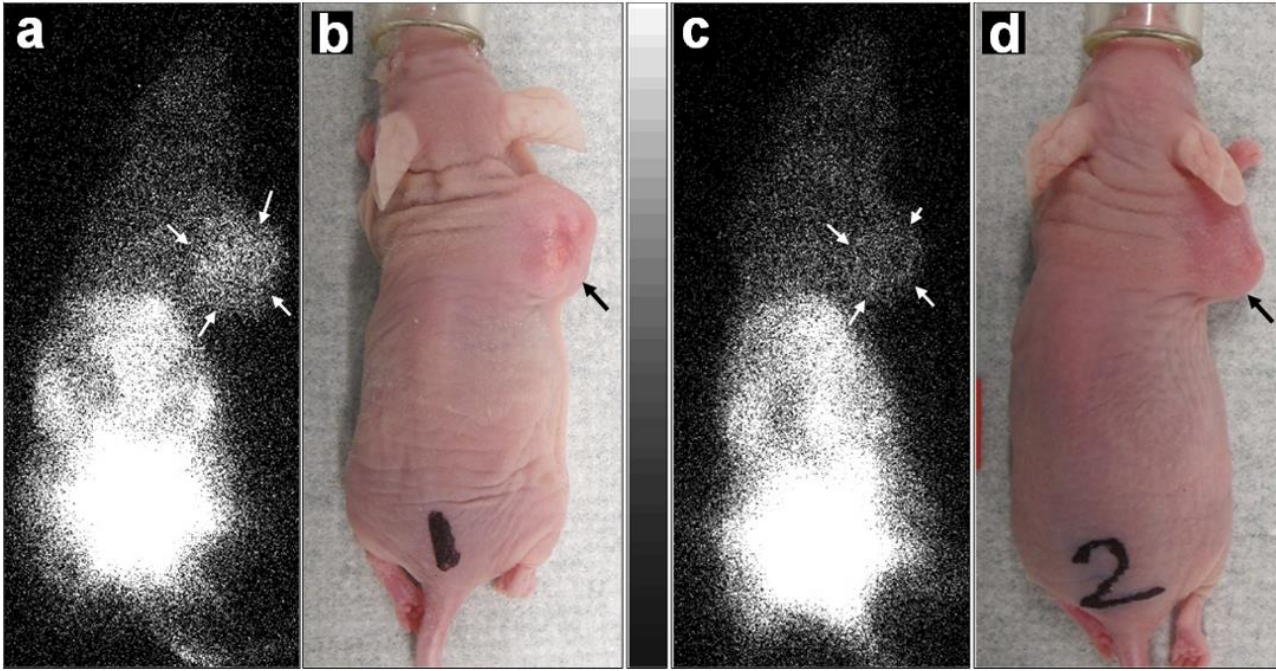
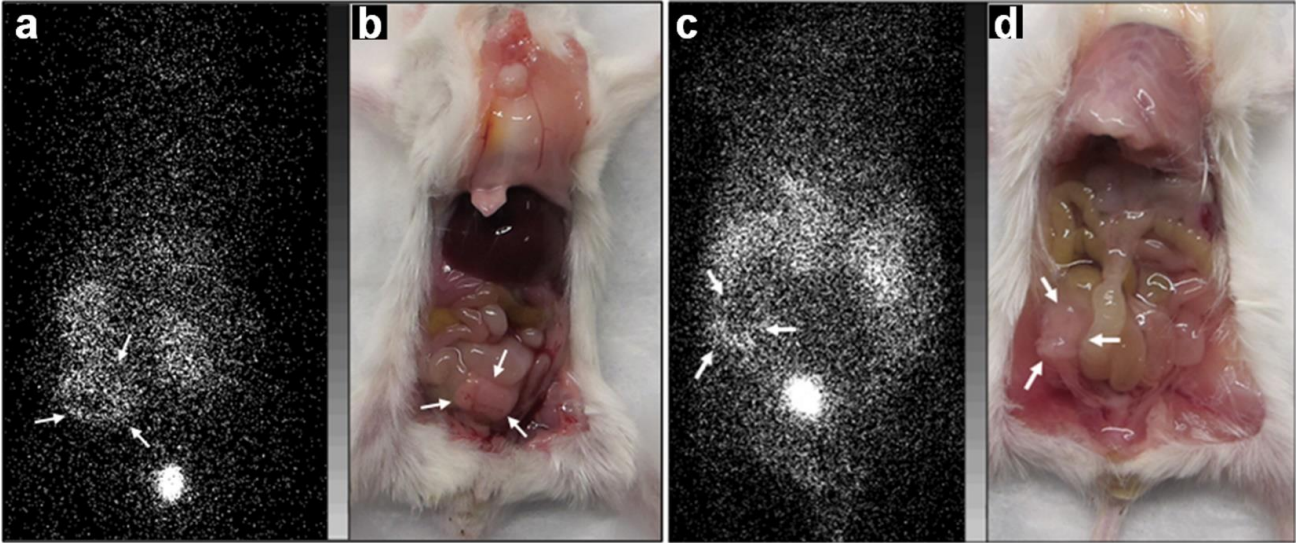


Figure 7



**Electronic Supplementary Material**

**PEGylated and non-PEGylated TCP-1 probes for imaging of colorectal cancer**

**Journal: *Molecular Imaging and Biology***

Zhonglin Liu,<sup>1,2\*</sup> Brian D Gray,<sup>3\*</sup> Christy Barber,<sup>1</sup> Li Wan,<sup>1</sup> Lars R Furenlid,<sup>1,4</sup> Rongguang Liang,<sup>4</sup> Zheng Li,<sup>2</sup> James M Woolfenden,<sup>1</sup> Koon Y Pak,<sup>3</sup> Diego R Martin,<sup>1,2</sup>

<sup>1</sup>Department of Medical Imaging at College of Medicine and <sup>4</sup>College of Optical Sciences, University of Arizona, Tucson, AZ

<sup>2</sup>Houston Methodist Research Institute, Houston Methodist Hospital, Houston, TX

<sup>3</sup>Molecular Targeting Technologies, Inc., West Chester, PA

**\* For correspondence or reprints contact:**

Email: [zliu2@houstonmethodist.org](mailto:zliu2@houstonmethodist.org) or [briangray@mtarget.com](mailto:briangray@mtarget.com)

### Synthesis of HYNIC-TCP-1 and HYNIC-PEG<sub>4</sub>-TCP-1

N-hydroxysuccinimide ester of HYNIC (**1**) was provided by Molecular Targeting Technologies, Inc. (West Chester, PA). HYNIC-TCP-1 (**2**) was prepared as shown in **Fig. S1** by reacting the terminal amino group of TCP-1 with (**1**) in the presence of 1-hydroxy-7-azabenzotriazole (HOAt) to accelerate the reaction. The coupled product was then purified by multiple injections on a semi-preparative C18 HPLC column (10mm x 250mm) and gradient elution with a water-acetonitrile + 0.1% trifluoroacetic acid (TFA) solvent system. Pure fractions were collected and lyophilized to provide 5.0 mg (40% yield). The material was characterized by analytical C18 HPLC for purity and mass spectroscopy to confirm identity. HYNIC-TCP-1 has molecular formula C<sub>50</sub>H<sub>66</sub>N<sub>14</sub>O<sub>14</sub>S<sub>2</sub>; M+H<sup>+</sup><sub>calc</sub> = 1152.3; M+H<sup>+</sup><sub>obs</sub> = 1151.8.

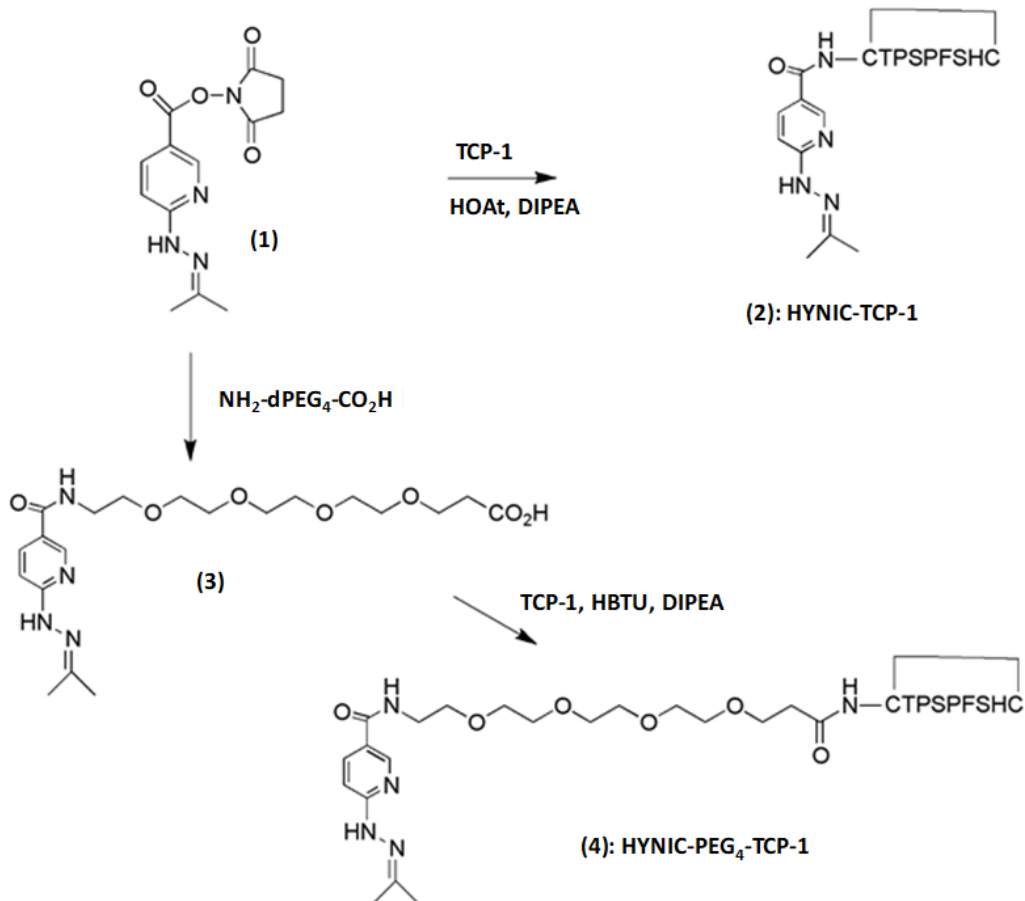


**Fig. S1.** Synthetic schemes to prepare HYNIC-TCP-1 and HYNIC-PEG<sub>4</sub>-TCP-1 precursors for labeling with <sup>99m</sup>Tc.

HYNIC-PEG<sub>4</sub>-TCP1 (**4**) was prepared as shown in **Fig. S1** by reacting the N-hydroxysuccinimide ester of HYNIC (**1**) first with amino-dPEG<sub>4</sub>-acid (Quanta BioDesign, Ltd., Plain City, Ohio) to provide intermediate (**3**) which was subsequently coupled with TCP-1 using the peptide coupling reagent, N,N,N',N'-tetramethyl-O-(1H-benzotriazol-1-yl)uranium hexafluorophosphate (HBTU). The coupled product was then purified by multiple injections on a semi-preparative C18 HPLC column as before and lyophilized to provide 4.5 mg (30% yield). The material was characterized by analytical C18 HPLC for purity and mass spectroscopy to confirm identity. HYNIC-PEG<sub>4</sub>-TCP-1 has molecular formula C<sub>61</sub>H<sub>87</sub>N<sub>15</sub>O<sub>19</sub>S<sub>2</sub>; M+H<sup>+</sup><sub>calc</sub> = 1399.6; M<sup>+</sup><sub>obs</sub>=1398.8.

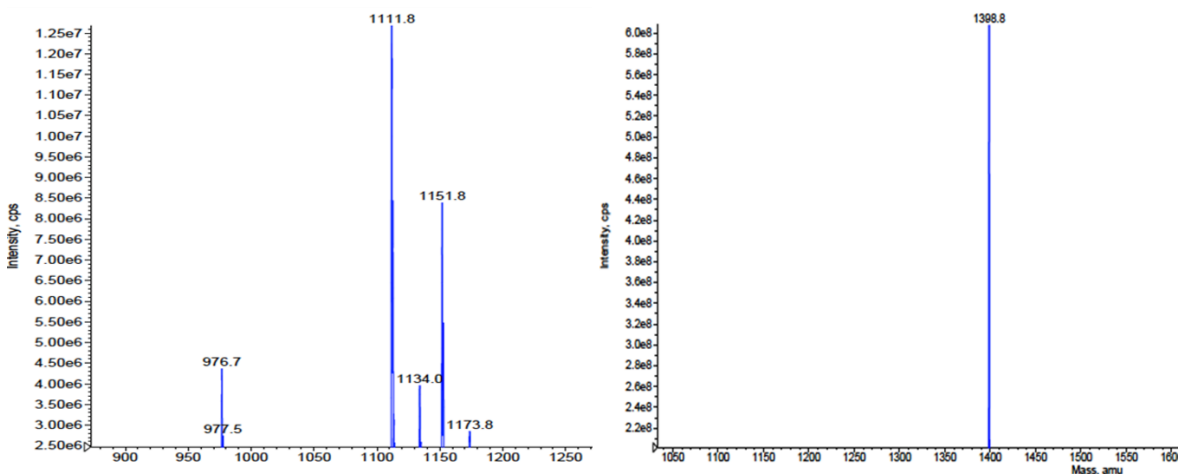


**Fig. S2.** Positive mode ion spray mass spectroscopic analysis of HYNIC-TCP-1 (*Left*) and HYNIC-PEG<sub>4</sub>-TCP-1 (*Right*) performed on a Sciex API-150 instrument.

The mass spectrum of HYNIC-TCP-1 product is shown in **Fig S2** and demonstrates the following mass peaks: the expected parent (M+H)<sup>+</sup> = 1151.8; (M+Na)<sup>+</sup> = 1173.8; (M+H-C<sub>3</sub>H<sub>4</sub>)<sup>+</sup> = 1111.8 (due to loss of labile acetone protecting group); (M-C<sub>3</sub>H<sub>4</sub>+ Na)<sup>+</sup>=1134; and 976.7 from TCP-1. No free TCP1 was observed in the sample by analytical HPLC, indicating the peak at 976.7 was due to a fragmentation occurring in the mass spec and not a TCP-1 impurity in the sample. The analytical HPLC profile of HYNIC-TCP-1 is shown in **Fig. S3** (top row), in which two peaks

at 22.2 min and 24.6 min correspond to HYNIC-TCP-1 minus the acetone hydrazone protecting group and HYNIC-TCP-1 respectively. The acetone hydrazone protecting group was eventually removed during the technetium labeling reaction, thus both protected and deprotected forms of HYNIC-TCP-1 provide the same radiolabeled product.

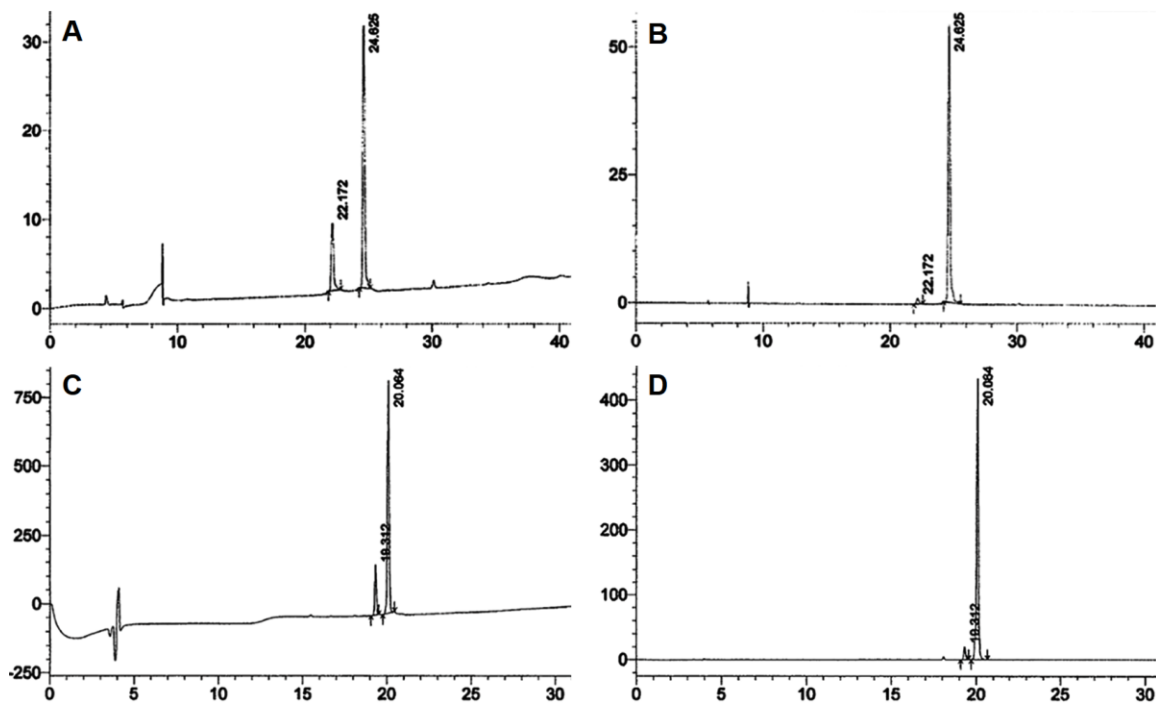


**Fig. S3.** HPLC chromatograms. HYNIC-TCP-1 at 330nm (A) and 220nm (B) detection; HYNIC-PEG<sub>4</sub>-TCP-1 at 330nm (C) and 220nm (D) detection. HPLC method consisted of a C18 column with solvent A (10% CH<sub>3</sub>CN in water + 0.1% TFA) and solvent B (CH<sub>3</sub>CN + 0.1% TFA) using a linear gradient of 0 to 45% B over 40 minutes at 1mL/min.

The mass spectrum of HYNIC-PEG<sub>4</sub>-TCP-1 is also presented in **Fig. S2** and shows the expected parent  $(M+H)^+ = 1398.8$  mass units. The analytical HPLC profile of the product after lyophilization is shown in **Fig. S3** (bottom row), in which two peaks at 19.3 min and 20.1 min correspond to the product of HYNIC-PEG<sub>4</sub>-TCP-1 with and without the acetone protecting group respectively, as seen in the profile of HYNIC-TCP-1. In comparison to the HYNIC-TCP-1, incorporation of the PEG<sub>4</sub> spacer enhanced the hydrophilicity of the HYNIC-PEG<sub>4</sub>-TCP-1

conjugate as evidenced by a shorter retention time on HPLC.

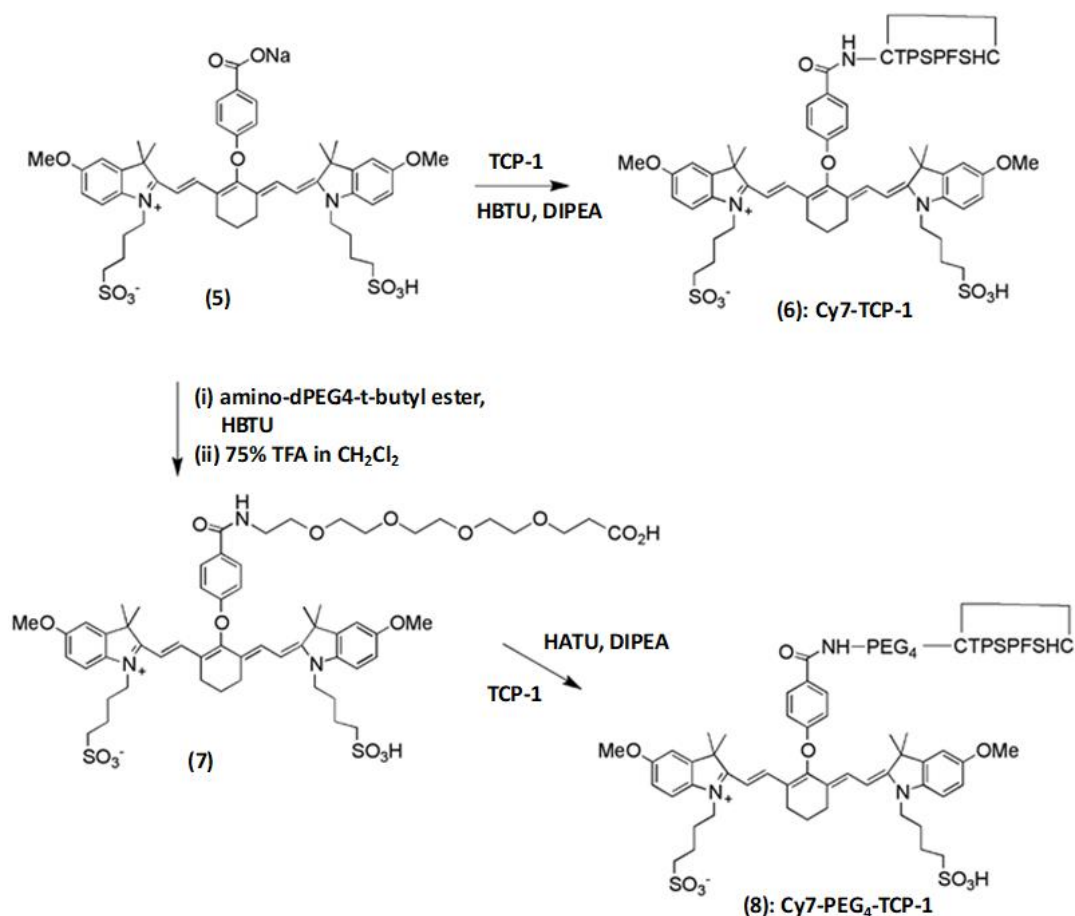


**Fig. S4.** Synthetic schemes to prepare near infrared fluorescent conjugates of TCP-1.

### *Synthesis of Cy7-TCP-1 and Cy7-PEG<sub>4</sub>-TCP-1*

Cy7-TCP-1 (**6**) was prepared as shown in **Fig. S4** by coupling the terminal amino group of TCP-1 with the Cy7 carboxylic salt (**5**) in the presence of HBTU. The coupled product was then purified by multiple injections on a semi-preparative C18 HPLC column (10mm x 250mm) and gradient elution with a water-acetonitrile + 0.1% TFA solvent system. Pure fractions were collected and lyophilized to provide 3.9 mg (21% yield). The material was characterized by analytical C18 HPLC for purity and mass spectroscopy to confirm identity. Cy7-TCP-1 has molecular formula  $C_{88}H_{110}N_{13}O_{23}S_4.Na$ ;  $(M+H)_{calc}=1847.4$ ,  $(M+H)_{obs}=1846.7$ .

Cy7-PEG<sub>4</sub>-TCP-1 (**8**) was prepared as shown in **Fig. S4** by coupling amino-dPEG<sub>4</sub>-t-butyl ester (Quanta BioDesign, Ltd., Plain City, Ohio) with (**5**) to provide an intermediate which was purified by column chromatography and subsequently treated with 75% TFA to provide carboxylic acid (**7**). TCP1 and (**7**) were coupled together using HBTU and the coupled product then purified by multiple injections on a semi-preparative C18 HPLC column as before and lyophilized to provide 5.1 mg (25% yield). The material was characterized by analytical C18 HPLC for purity and mass spectroscopy to confirm identity. Cy7-PEG<sub>4</sub>-TCP-1 has molecular formula C<sub>99</sub>H<sub>131</sub>N<sub>14</sub>O<sub>28</sub>S<sub>4</sub>.Na; (M+H)<sub>calc</sub>= 2094.4, (M+H)<sub>obs</sub>= 2094.1.

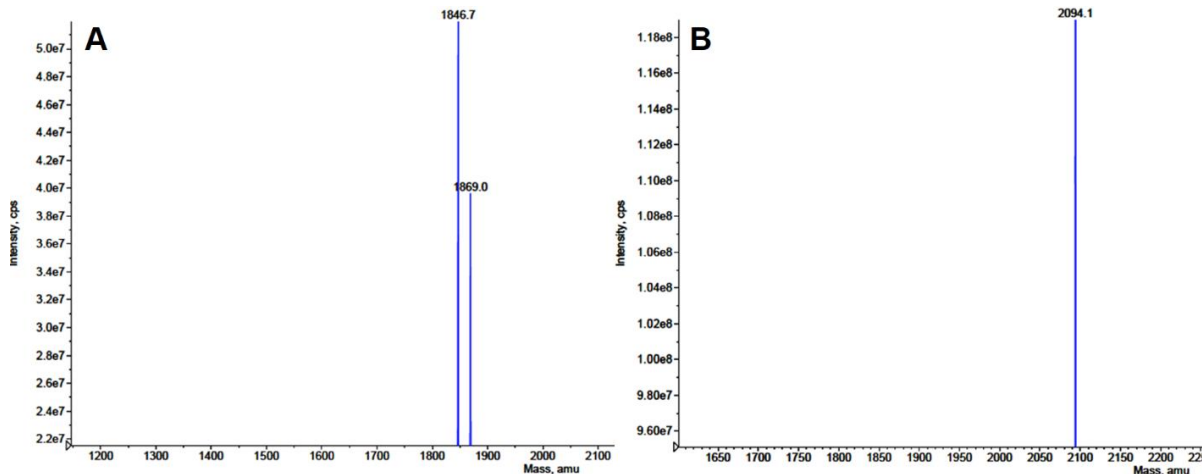


**Fig. S5.** Positive mode ion spray mass spectroscopic analysis of Cy7-TCP-1 (**A**) and Cy7-PEG<sub>4</sub>-TCP-1 (**B**) performed on a Sciex API-150 instrument.

The mass spectrum of Cy7-TCP-1 demonstrated a peak for the expected parent M+H = 1846.7 and also for (M+Na)<sup>+</sup> = 1869 as shown in **Fig. S5A**. In contrast, Cy7-PEG<sub>4</sub>-TCP-1 mass spectrum exhibited the expected parent M+H = 2094.1 mass units (**Fig S5B**). The analytical HPLC profiles of Cy7-TCP-1 and Cy7-PEG<sub>4</sub>-TCP-1 are presented in **Fig. S6**, which show a main peak at 794 nm with retention time of 25.5 min for both and purity of 86% and 98.6%, respectively. Thus, chromatography of purified Cy7-TCP-1 and Cy7-PEG<sub>4</sub>-TCP-1 revealed successful removal of unreacted Cy7. HPLC retention times of Cy7-TCP-1 and Cy7-PEG<sub>4</sub>-TCP1 were almost

identical under the same HPLC conditions suggesting incorporation of the PEG<sub>4</sub> spacer had minimal effect on the overall hydrophilicity of the conjugate. The absorption and fluorescence emission characteristics of Cy7-TCP-1 and Cy7-PEG<sub>4</sub>-TCP-1 conjugates were similar to those of free Cy7, suggesting that the fluorescence property of Cy7 was not affected by conjugation reaction.

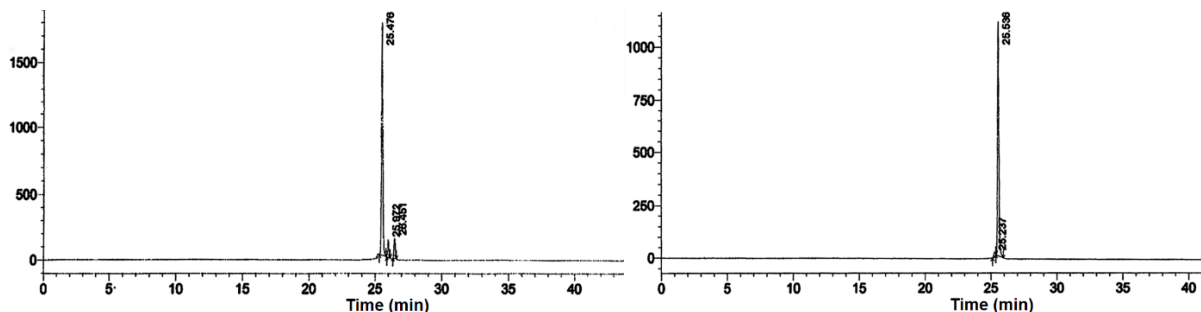


**Fig. S6.** HPLC chromatograms of Cy7-TCP-1 (*Left*) and Cy7-PEG<sub>4</sub>-TCP-1 (*Right*) at 794nm detection. HPLC method consisted of a C18 column with solvent A (10% CH<sub>3</sub>CN in water + 0.1% TFA) and solvent B (CH<sub>3</sub>CN + 0.1% TFA) using a linear gradient of 0 to 70% B over 40 minutes at 1mL/min.

### ***Radiolabeling TCP-1 conjugates with <sup>99m</sup>Tc***

Radiolabeling took place by adding pertechnetate (<sup>99m</sup>TcO<sub>4</sub><sup>-</sup>) in saline (370-555 MBq, 0.5 mL) to the vial containing 15 μg of HYNIC-TCP-1 or HYNIC-PEG<sub>4</sub>-TCP-1 30 mg of tricaine, 10 mg of EDDA, and 15 μg of tin chloride dihydrate. The mixture was incubated for 30 minutes at 80°C. Radiolabeled products, [<sup>99m</sup>Tc]Tc-HYNIC-TCP-1 and [<sup>99m</sup>Tc]Tc-HYNIC-PEG<sub>4</sub>-TCP-1 were purified by reverse-phase (RP) HPLC using a C18 column with a gradient elution of 0.1% trifluoroacetic acid (TFA) in water for the A-solvent and 0.1% TFA in acetonitrile (ACN) for the B-solvent at a flow rate of 1 mL/min. After HPLC purification, radiochemical purity (RCP) was greater than 99% for animal administration within 1 hour.

The labeling yield of the product was 92-95% and the radiochemical purity was greater than 99% after HPLC purification. Representative HPLC radiochromatogram of [<sup>99m</sup>Tc]Tc-

HYNIC-PEG<sub>4</sub>-TCP-1 is shown in **Fig. S7A**. The retention times were 5.12 minutes for <sup>99m</sup>TcO<sub>4</sub><sup>-</sup> and 16.64 minutes for [<sup>99m</sup>Tc]Tc-HYNIC-PEG<sub>4</sub>-TCP-1. After 1 hour and 6 hours of incubation at 37°C, more than 98% and 95% of [<sup>99m</sup>Tc]Tc-HYNIC-TCP-1, respectively, remained intact in saline or mouse serum, as shown in **Fig. S7B** and **Fig. S7C**. The major species produced in plasma was <sup>99m</sup>TcO<sub>4</sub><sup>-</sup>, with a retention time of approximately 5 minutes. Its identity was confirmed by a retention time identical to that of authentic sodium <sup>99m</sup>Tc-pertechnetate. There was no evidence of any metabolism occurring in serum.

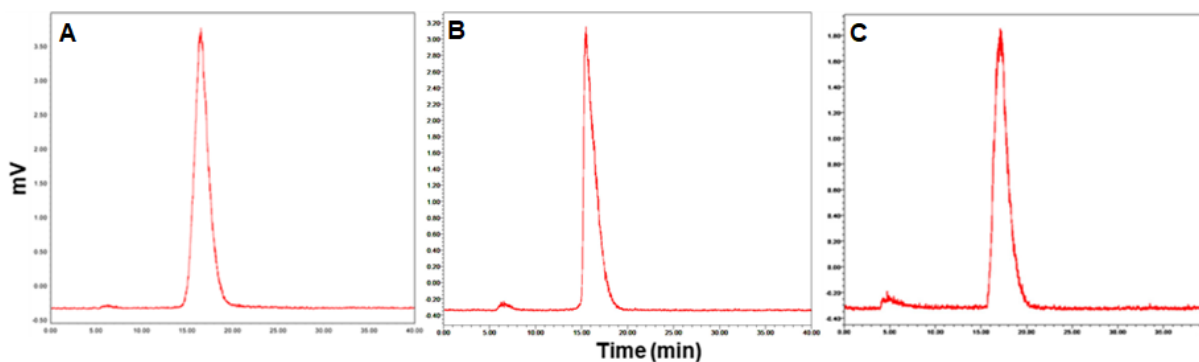


**Fig. S7.** Representative HPLC radiochromatograms of [<sup>99m</sup>Tc]Tc-HYNIC-TCP-1 immediately after purification in saline (**A**) and after incubation at 37°C in mouse serum for 3 hours (**B**) and 6 hours (**C**).